

# Dalton Transactions

Accepted Manuscript



This is an *Accepted Manuscript*, which has been through the Royal Society of Chemistry peer review process and has been accepted for publication.

*Accepted Manuscripts* are published online shortly after acceptance, before technical editing, formatting and proof reading. Using this free service, authors can make their results available to the community, in citable form, before we publish the edited article. We will replace this *Accepted Manuscript* with the edited and formatted *Advance Article* as soon as it is available.

You can find more information about *Accepted Manuscripts* in the [Information for Authors](#).

Please note that technical editing may introduce minor changes to the text and/or graphics, which may alter content. The journal's standard [Terms & Conditions](#) and the [Ethical guidelines](#) still apply. In no event shall the Royal Society of Chemistry be held responsible for any errors or omissions in this *Accepted Manuscript* or any consequences arising from the use of any information it contains.

# Dipyrrolylquinoxaline Difluoroborates with Intense Red Solid-State Fluorescence

*Changjiang Yu, Erhong Hao\*, Tingting Li, Jun Wang, Wanle Sheng, Yun Wei, Xiaolong Mu and Lijuan Jiao\**

The Key Laboratory of Functional Molecular Solids, Ministry of Education; Anhui Laboratory of Molecule-Based Materials; School of Chemistry and Materials Science, Anhui Normal University, Wuhu, Anhui, China 241000.

\*To whom correspondence should be addressed. E-mail: [haoehong@mail.ahnu.edu.cn](mailto:haoehong@mail.ahnu.edu.cn),

[jiao421@mail.ahnu.edu.cn](mailto:jiao421@mail.ahnu.edu.cn)

## Abstract

A set of organic fluorescent dyes of dipyrrolylquinoxalines (PQs **4-6**) and their BF<sub>2</sub> complexes (BPQs **1-3**) were synthesized from commercial reagents, and were characterized by their X-ray structural analysis, and optical and electrochemical properties. BPQs **1-3** showed intensely broad absorption in the visible region in solution-state. In comparison with that of PQs **4-6**, there is an over 110 nm red-shift of the absorption maximum in these BPQs **1-3** (up to 583 nm). Interestingly, dyes **1-6** all exhibit red solid-state fluorescence with moderate to high fluorescence quantum yields except PQ **4** which showed bright yellow solid-state fluorescence. X-ray structures of BPQs **2-3** showed the planar structure of quinoxaline with one pyrrole unit via the BF<sub>2</sub> chelation and the almost perpendicular orientation of uncoordinated pyrrole to the NBN core plane (the dihedral angle of 70-73°). The extended  $\pi$ -conjugation was in good agreement with the observed red-shift of the spectra. These dyes formed well-

ordered intermolecular packing structures via the intermolecular hydrogen bonding between the N atoms of quinoxaline moieties and the NH units of adjacent pyrroles. The lacking of  $\pi$ - $\pi$  stacking in their crystal packing structures may explain the interestingly intense solid-state fluorescence of these dyes.

## Introduction

Organic fluorescent dyes have found wide applications in biomedical and material science, for example as organic light-emitting diodes (OLED), solid-state organic lasers, bio-molecular labels and molecular probes.<sup>1</sup> Boron complexation has been documented as an efficient strategy to enhance the rigidity and the fluorescence intensity of the molecules, and many organoboron complexes have been used as organic solid-state fluorescent dyes in optoelectronics.<sup>1-2</sup> However, some organoboron complexes suffer from the quenching of the fluorescence at high concentration or in solid state. For example, BODIPY (A in Figure 1) dyes,<sup>3</sup> as one of the most popular and intriguing dyes have been extensively studied in the last two decades due to their outstanding chemical and photophysical properties, such as the strong absorption in the visible and NIR region, high fluorescent quantum yield and excellent photochemical stability, while they show very small Stokes shifts and extremely low fluorescence in concentrated solution or solid-state. In addition, most of those reported solid emitting dyes that reached to the red region generally showed quite low fluorescence quantum yields.

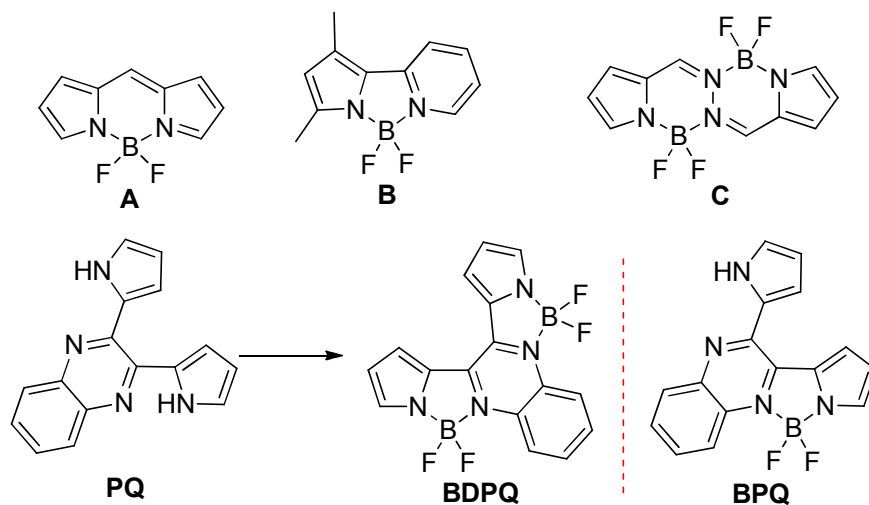


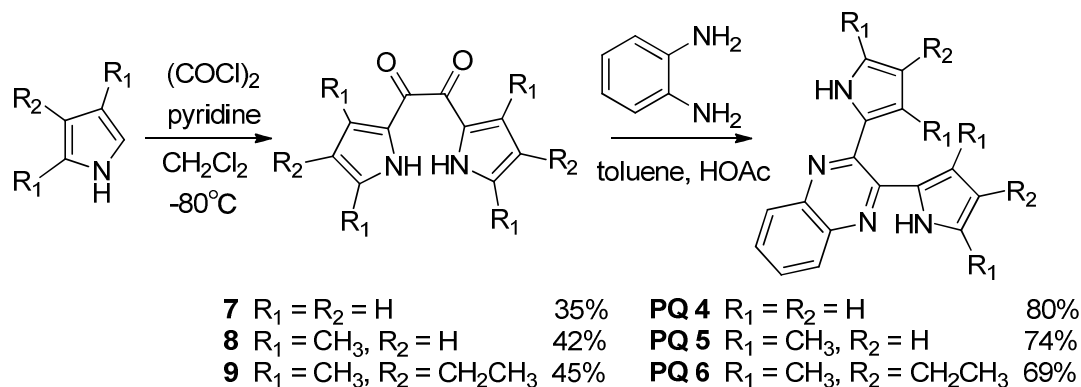
**Fig. 1.** Chemical structures of BODIPY core (A), pyrrolylpyridine BF<sub>2</sub> scaffold (B), the BF<sub>2</sub> complex of hydrazine-linked bispyrrole (C), and the dipyrrolylquinoxaline (PQ) and the two possible BF<sub>2</sub> complexes of PQ (BDPQ and BPQ).

Some lately elegant researches on the desymmetrical bidentate nitrogen ligands<sup>2,4-5</sup> have already

demonstrated the essential roles of suitable ligands in the development of novel (family of) fluorescent dyes with a set of desired properties, like the large Stokes-shift and the high solid-state fluorescence addressed here. As part of our effort toward large Stokes-shift and highly fluorescent solid materials, we recently have designed a hydrazine-linked bispyrrolic ligand **C**<sup>6</sup> upon BF<sub>2</sub> complexation, which shows improved Stokes-shift up to around 70 nm over comparable BODIPY dyes and high solid-state fluorescence. Noticed that a set of dipyrrolylquinoxaline (PQ, Figure 1) derivatives have been developed by Oddo and Behr and have recently been applied as colorimetric anion sensors by Sessler and coworkers<sup>7, 8</sup>, while few efforts have been devoted to the investigation of their fluorescence properties.<sup>9</sup> Besides, the BF<sub>2</sub> complexes of pyrrolylpyridines<sup>10</sup> (**B**, Figure 1) show large Stokes-shift (up to 100 nm) and acceptable fluorescent quantum yield ( $\phi = 0.22$  in THF) with strong absorption in the ultra violet region ( $\lambda_{\text{abs}}^{\text{max}} = 325$  and 405 nm). Taking the structural advantage of PQ derivatives (possessing both the pyrrolic NH unit and the aromatic quinoxaline N atom), we rationalized that the BF<sub>2</sub> complexation of suitable PQ derivatives would render the desired red-shift of the absorption spectra with the extended conjugation via the annulation of an benzene moiety onto the chromophore, while maintain the large Stokes-shift due to the asymmetrical structure of the complex. Herein, we report the efficient synthesis of a set of BF<sub>2</sub> complexes of PQ (BPQs **1-3**) with intense red solid-state fluorescence, and the comparatively investigation of their X-ray structures, optical and electrochemical properties of these dyes with their corresponding PQ ligands.

## Results and Discussion

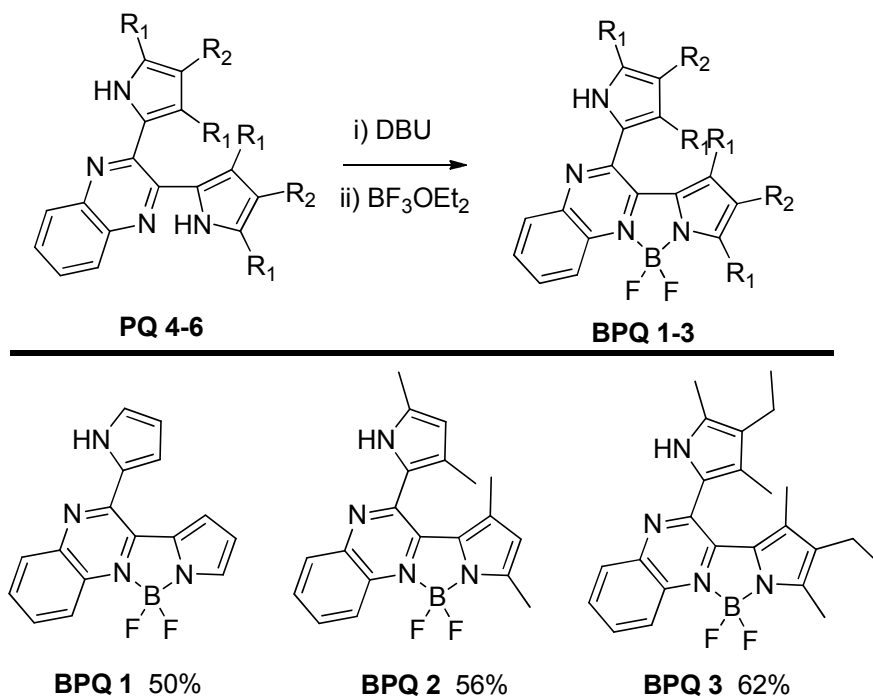
Dipyrrolyldiketones **7-9** as the key synthetic precursor for PQs **4-6** were prepared in 35%-45% yields using a literature procedure<sup>7a, 8a</sup> via the condensation of oxalyl chloride with a stoichiometric amount of commercial pyrrole, 2,4-dimethylpyrrole or 3-ethyl-2,4-dimethylpyrrole in the presence of dry pyridine (Scheme 1). These resultant dipyrrolyldiketones were applied for the subsequent condensation with excess amount of 1,2-phenylenediamine by following a modified literature procedure<sup>7, 8</sup>, from which the target PQs **4-6** were prepared in 69%-80% yields.



**Scheme 1.** Syntheses and yields of dyes PQs 4-6.

Our initial attempt to form the  $BF_2$  complex of PQ **4** using triethylamine as the base produced only tiny amount of product, from which most of PQ **4** was recovered. When 1, 8-diazabicyclo[5.4.0]undec-7-ene (DBU) was used as the base, the  $BF_2$  complexation of PQ **4** was smoothly proceeded in toluene under refluxing condition, from which a major product was obtained in 50% isolated yield (Scheme 2). Theoretically, there are two possible products for the five-member-ring  $BF_2$  complexation (Figure 1): the mono-chelated BPQ and the dichelated BDPQ. The major product from this reaction was confirmed by the X-ray diffraction to be BPQ **1**. No BDPQ was isolated from this reaction with the variation of the reaction conditions, including the further increasing of the amount of boron trifluoride etherate ( $BF_3 \cdot OEt_2$ ) and the usage of a stronger base. This may result from the poor stability of BDPQ which readily undergoes decomposition upon formation.<sup>11</sup>

To test the versatility of this reaction and to facilitate the further investigation of the substituent effect on the optical and electronic properties of the resultant dyes, we further extended this reaction condition to the  $BF_2$  complexation of PQs **6-7**, from which the desired BPQs **2** and **3** was smoothly generated in 56% and 62% yields, respectively and were full characterized by HRMS, NMR and single crystal structural analysis.



**Scheme 2.** Syntheses and yields of BPQs 1-3.

As shown in Figure 2a and summarized in Table 1, PQs 4-6 each showed intense absorption centered at the range of 410-450 nm with high extinction coefficients (up to  $4.18 \times 10^4 \text{ M}^{-1}\text{cm}^{-1}$ ) in dichloromethane. Their fluorescence emission centered at around 490-550 nm in dichloromethane with fluorescence quantum yield between 0.13 and 0.20 (Figure 2b). Under daylight irradiation condition, their dichloromethane solutions show a pale yellow color, which changes to an intense blue for PQ 4 and light green for PQs 5-6 under handheld UV lamp irradiation (365 nm) condition (Figure 2c).

BPQ 1 gave a broad absorption band centered at 492 nm with two shoulders at around 465 and 520 nm in dichloromethane in the visible region and a comparably high extinction coefficient ( $4.27 \times 10^4 \text{ M}^{-1}\text{cm}^{-1}$ ) to most organoboron complexes. In comparison with that of PQ 4, there is an approximately 80 nm red-shift of the absorption in BPQ 1 (Figure 2). Similar absorption patterns in the visible region were observed for BPQs 2 and 3 containing electron-donating alkyl substituents in dichloromethane with the absorption maximum centered at 529 and 547 nm, respectively (Figure 2).

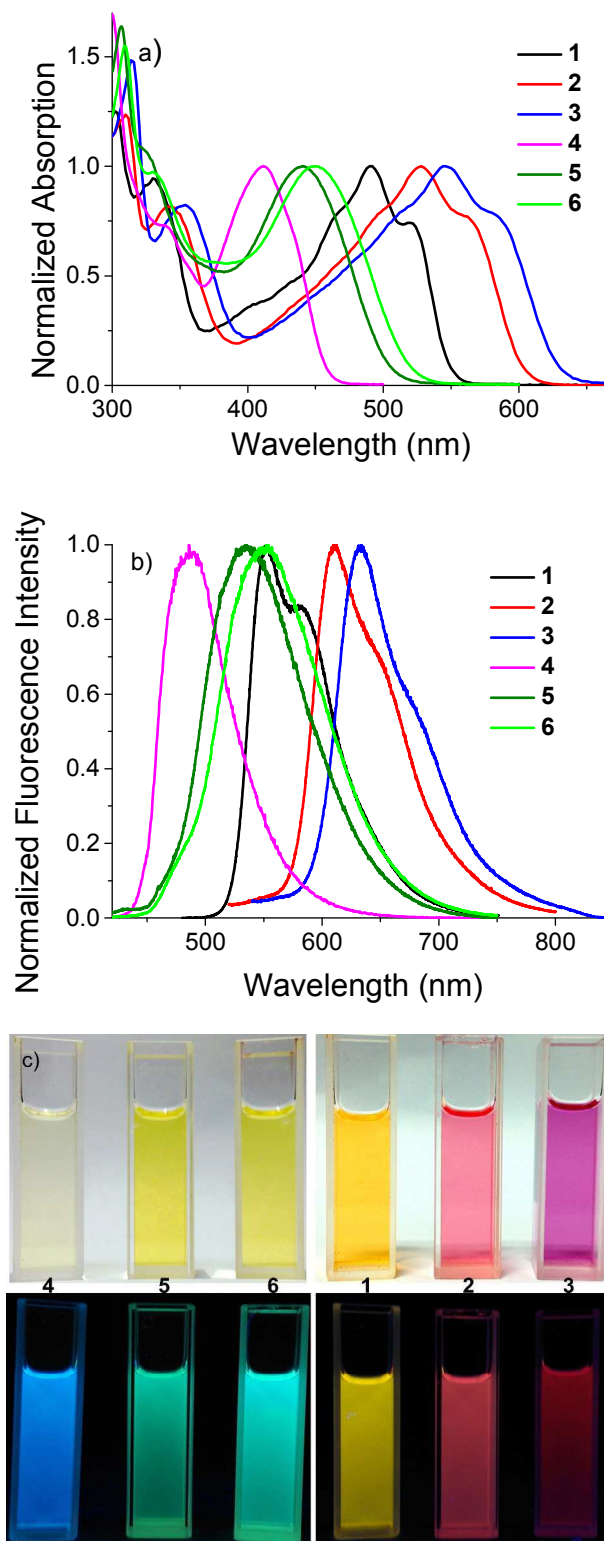


**Fig. 2.** Overlaid and normalized absorption (a), fluorescence emission (b) spectra and the colors (c) of the dichloromethane solutions of dyes **1-6** under daylight (top) and a handheld UV lamp irradiation (365 nm) (bottom) conditions.

BPQs **1-3** showed their fluorescence emission maximum centered at the range of 490-550 nm in



dichloromethane with fluorescence quantum yields between 0.07 and 0.23. In comparison with that of BPQ **1**, a significant red-shift of the fluorescence emission was also observed in BPQs **2-3**: BPQ **1** showed fluorescence emission maximum centered at 552 nm with a shoulder at 583 nm in dichloromethane, while fluorescence emission maximum of BPQ **3** was red-shifted to 632 nm with a shoulder extended to 675 nm. Similar red-shifts of the fluorescence emission were also observed in other solvents (Table 1).

Under daylight irradiation condition, the dichloromethane solutions are pale yellow for BPQ **1**, pink for BPQ **2** and purple for BPQ **3** respectively. The same colors were observed for BPQs **1-2** under handheld UV lamp irradiation condition, while a red solution color was observed for BPQ **3** in this condition (Figure 2c).

The solvent-dependent optical properties for BPQs **1-3** was investigated and was summarized in Table 1 and Figures S1-S6 in the Supporting Information. The fluorescence emission maximum of these dyes varies with the variation of the solvent polarity from hexane to acetonitrile. A gradual decrease of the fluorescence quantum yields was observed for BPQs **1-3** with the increase of the solvent polarity. For example, the fluorescence quantum yields for BPQ **3** were reduced from 0.18 to 0.13, 0.07 and 0.04 with the increasing of the solvent polarity from hexane to toluene, dichloromethane and acetonitrile. This may be attributed to the strong intramolecular charge transfer (ICT) process<sup>12</sup> from uncoordinated pyrroles to the BF<sub>2</sub> complex of pyrrolylquinoxaline moiety in BPQs **1-3**. In addition, a pH sensitive absorption was also observed for BPQs **1-3**. A red-shift of absorption maximum in the visible region was observed with the addition of TFA to the dichloromethane solutions of these dyes (Figures S4-6 in Supporting Information) resulted from the protonation of lone pairs of the nitrogen atom in quinoxaline unit.

Table 1. Photophysical properties of dyes **1-6** in various solvents studied and in solid-state at room temperature.

	solvents	$\lambda_{\text{abs}}^{\text{max}}$ (nm) ( $\log \epsilon_{\text{max}}$ ) <sup>a</sup>	$\lambda_{\text{em}}^{\text{max}}$ (nm)	Stokes-shift (nm)	$\phi_{\text{f}}$ <sup>b</sup>
<b>1</b>	hexane	304(4.33), 330(4.20), 470(3.73), 492(4.27), 528(4.22)	536, 555, 574	63	0.39
	toluene	301(4.31), 334(4.16), 467(3.71), 494(4.23), 526(4.12)	552, 581(sh)	58	0.28
	dichloromethane	304(4.31), 332(4.19), 465(3.77), 492(4.22), 520(4.09)	552, 583(sh)	60	0.23
	acetonitrile	301(4.32), 326(4.19), 484(4.22)	556	72	0.04
	solid	300-650	636	-	0.09
<b>2</b>	hexane	311(4.78), 345(4.59), 495(3.99), 521(4.69), 558(4.62)	588, 634	67	0.33
	toluene	310(4.72), 346(4.51), 495(4.04), 527(4.66), 564(4.57)	600, 636(sh)	73	0.13
	dichloromethane	311(4.74), 344(4.56), 496(4.17), 529(4.65), 562(4.14)	611, 648(sh)	82	0.10
	acetonitrile	309(4.74), 339(4.52), 521(4.63)	600	79	0.05
	solid	300-670	664	-	0.21
<b>3</b>	hexane	314(4.60), 355(4.36), 507(3.84), 537(4.45), 577(4.37)	611, 656(sh)	74	0.18
	toluene	316(4.57), 355(4.30), 510(3.84), 544(4.44), 583(4.34)	622, 666(sh)	78	0.13
	dichloromethane	316(4.58), 353(4.33), 511(3.92), 547(4.40), 582(3.94)	632, 675(sh)	85	0.07
	acetonitrile	314(4.58), 347(4.26), 539(4.39)	622	83	0.04
	solid	300-670	665	-	0.19
<b>4</b>	dichloromethane	300(5.12), 340(3.61), 412(4.18)	487	75	0.19
	solid	300-530	532	-	0.13
<b>5</b>	dichloromethane	307(4.83), 325(4.12), 440(3.99)	535	95	0.20
	solid	300-670	614	-	0.09
<b>6</b>	dichloromethane	309(4.89), 331(4.08), 450(4.12)	552	102	0.13
	solid	300-620	603	-	0.16

<sup>a</sup>Molar absorption coefficients are corresponding to the maximum absorption of the dye. <sup>b</sup>The absolute quantum yields ( $\phi_{\text{f}}$ ) are determined using Edinburgh Instrument FLS920 spectrofluorimeter by calibrating sphere systems, excited at 500 nm for **1**, at 520 nm for **2** and **3**, and at 400 nm for **4-6**. All  $\phi_{\text{f}}$  values are corrected for changes in refractive indexes of different solvents. The standard errors are less than 5%.

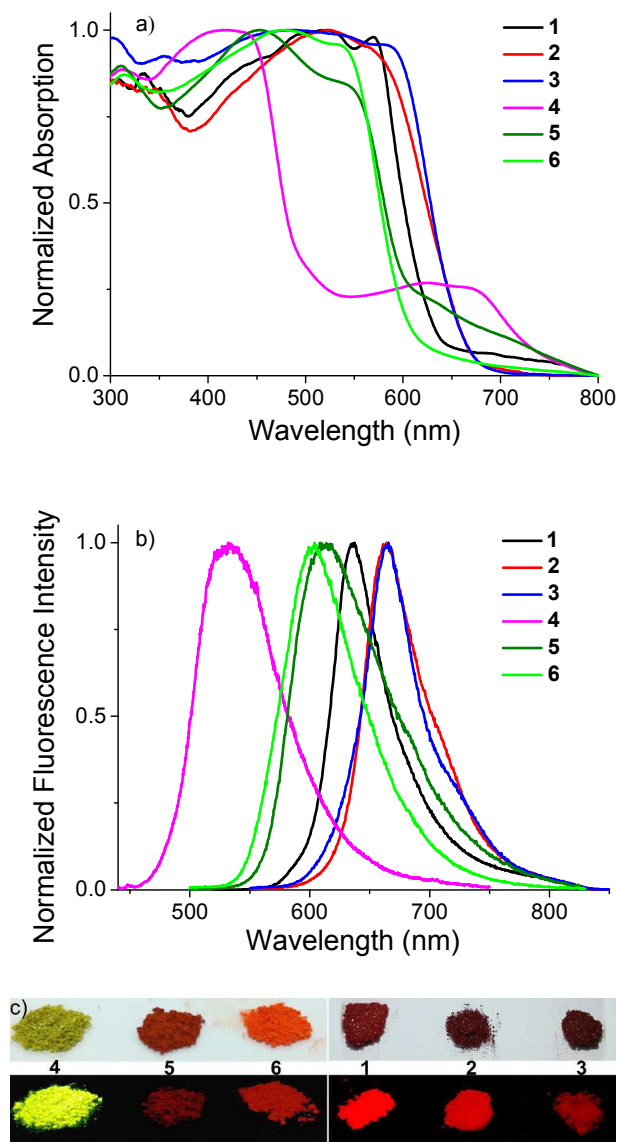


**Fig. 3.** Normalized absorption (a), fluorescence emission (b) spectra and the powder fluorescence images under daylight (top) and a handheld UV (365 nm) lamp (bottom) irradiation condition (c) of BPQs 1-6.

As shown in Figure 3 and Table 1, powders of BPQs 1-3 showed strong broad solid-state absorption in the UV-visible region and intense solid-state fluorescence emission (centered at 636, 654 and 655 nm, respectively) with the absolute fluorescence quantum yields of 0.09, 0.21 and 0.19, respectively. Notably, PQs 4-6 each showed intense solid-state fluorescence emission maximum centered at 532, 614 and 603 nm, respectively with a comparable solid-state fluorescent quantum yield (0.13, 0.09 and 0.16, respectively). In comparison with their solution-state, a red-shift was observed in the solid-state

fluorescence emission maximum for these dyes (Table 1). Under daylight irradiation condition, PQs **4-6** each showed a dark yellow, brown and orange color respectively, which changed into orange, dark red and brown colors accordingly under handheld UV lamp irradiation condition (Figure 3c). By contrast, deep red colors were observed for the powders of BPQs **1-3** under daylight irradiation condition, which changed into an intense bright red color under handheld UV lamp irradiation condition. This may result from the aggregation-induced CT states<sup>13</sup> and makes dyes **1-6** ideal bright yellow and red solid emitting materials.

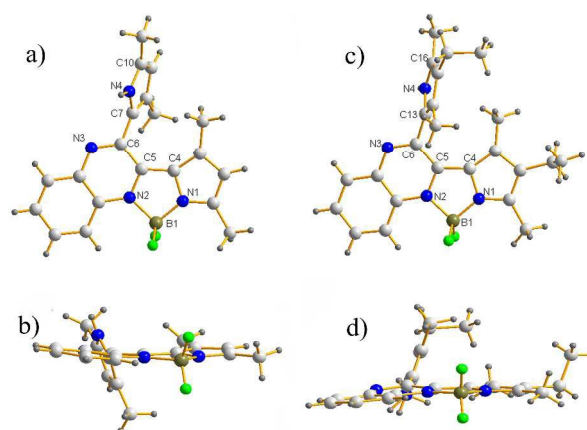


**Fig. 4.** Top view (a, c) and front view (b, d) of the X-ray structures of BPQs **2** and **3**. C, light gray; H, gray; N, blue; B, dark yellow; F, green.

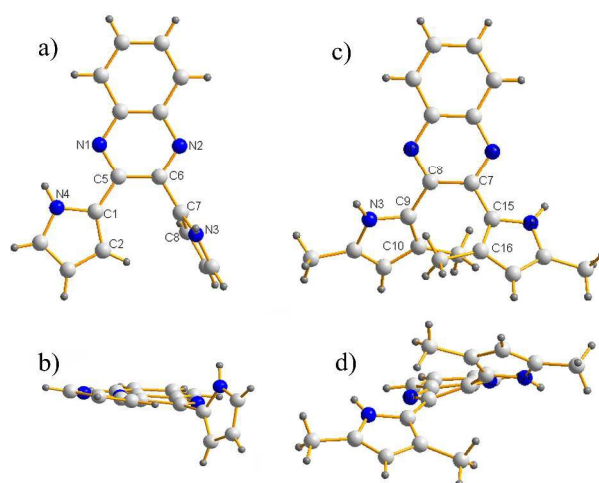


**Fig. 5.** Top view (a, c) and front view (b, d) of X-ray structures of PQs **4** and **5**. C, light gray; H, gray;

N, blue.

For a better understanding of the strong solid-state fluorescence of these dyes, the crystal structures of these dyes and their packing features were investigated and the crystal parameters were summarized in Table S1 in the supporting information. Crystals of BPQs **2**, **3** and PQs **4**, **5** suitable for X-ray analysis were obtained via the slow diffusion of hexane into their dichloromethane solutions (Figures 4 and 5). As shown in Figure 4, both BPQs **2** and **3** contain a almost planar NBN core structure formed between a pyrrole and the quinoxaline unit via the BF<sub>2</sub> chelation, in which a small dihedral angle was observed between these two moieties (10.1° for BPQ **2** and 6.3° for BPQ **3**, respectively). The other uncoordinated pyrrole in these two dyes stays almost perpendicular to this NBN core (dihedral angle of 66.1° for BPQ **2** and 68.7° for BPQ **3**, respectively). The boron atoms of BPQs **2** and **3** both showed a tetrahedral geometry and the plane defined by F-B-F atoms is almost perpendicular to that of the NBN core structure of these two dyes. The B1-N1 bond distances of BPQs **2** and **3** (1.53 Å, 1.51 Å, respectively) are about 0.08 Å shorter than their B1-N2 bond distance (1.61 Å, 1.59 Å), which indicates the asymmetrical structure features of these molecules.

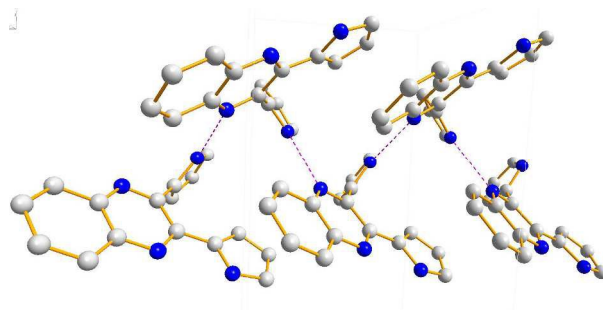


**Fig. 6.** Crystal-packing patterns of PQ **4** that shows the lacking of  $\pi$ - $\pi$  stacking between the adjacent interlayered crystals; C, light gray; H, gray; N, blue. Intermolecular N-N: 3.08 Å; Intramolecular N-N: 2.68 Å and 3.24 Å. Hydrogen atoms have been removed for clarity.

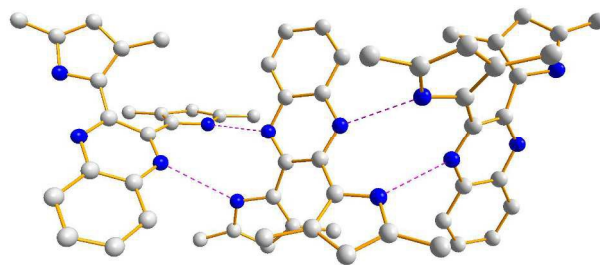


**Fig. 7.** Crystal-packing pattern of PQ **5** that shows the lacking of  $\pi$ - $\pi$  stacking between the adjacent interlayered crystals. C, light gray; H, gray; N, blue. Intermolecular N-N: 2.98 Å, 3.01 Å, 3.05 Å; Intramolecular N-N: 2.79 Å and 2.82 Å. Hydrogen atoms have been removed for clarity.

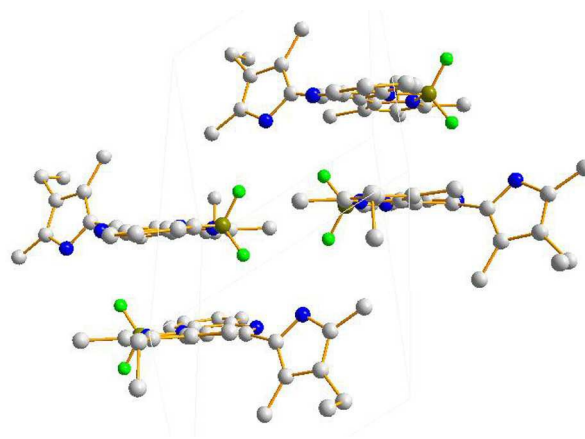


**Fig. 8.** Crystal-packing pattern of BPQ **3** that shows the lacking of  $\pi$ - $\pi$  stacking between the adjacent interlayered crystals; C, light gray; N, blue; B, dark yellow; F, green. Hydrogen atoms have been removed for clarity.

Multiple intramolecular and intermolecular C-H $\cdots$ F hydrogen bonds between F atoms and various hydrogen atoms are formed in BPQs **2-3** due to the strong electron negativity of the F atom. The strong intermolecular hydrogen bonding also helps the establishment of the crystal packing structures of these dyes in solid-state (Figure 8 and Figures S7 in the Supporting Information). Slipped “head to tail” dimers are formed in crystal packing structure of **3** (Figures 8). The plane of the two molecules are almost parallel (angle between the mean planes of the C<sub>2</sub>N<sub>2</sub> cores is 0.0°). The mean distance between the planes of two neighboring core is 3.96 Å. Further packing of these dimers was achieved via hydrogen bondings, and no  $\pi$ - $\pi$  stacking between the adjacent dimers was observed in these dyes.

This typical *J*-aggregate type packings<sup>14</sup> of BPQs **2** and **3** might explain their good fluorescence quantum yields in the solid-state.

PQs **4** and **5** both showed a slightly different inverted conformation for the two pyrrole rings with NH of each pyrrole pointing toward the quinoxaline nitrogen atoms (Figure 5). For PQ **5**, the dihedral angles between the two pyrrole and quinoxaline units are similar (35.6° and 40.7°, respectively). In addition, the intramolecular N-N bond lengths between the N atoms of quinoxaline and the two NH on the adjacent pyrroles are also similar (2.79 Å and 2.82 Å, respectively). By contrast, the two pyrrole rings on PQ **4** took different spatial orientation with one pyrrole nearly coplanar (dihedral angle of 5.6°) while the other pyrrole almost orthogonal (dihedral angle of 86.1°) to the quinoxaline plane. A different intramolecular N-N bond lengths (2.68 Å and 3.24 Å, respectively) were observed between the N atoms of quinoxaline and the NH of the two adjacent pyrroles. These conformational differences induce a remarkable difference in the crystal packing structures of PQs **4** and **5** (Figures 6 and 7). For PQ **5**, both pyrroles participate in the hydrogen bonding with their neighboring quinoxaline molecules with a mean distance of 3.01 Å. These hydrogen bondings lead to an extended two-dimensional array packing structure for PQ **5**. By contrast, only the orthogonal pyrrole in PQ **4** participates in the hydrogen bonding with its neighboring quinoxaline molecule with the distances of 3.08 Å, while the other pyrrole coplanar to quinoxaline moiety only participates in an intramolecular hydrogen bonding with quinoxaline (the distances of 2.68 Å). In both cases, no  $\pi$ - $\pi$  stacking was observed for these PQ dyes which may explain the interestingly strong solid fluorescence of these dyes.

Finally, the electronic states (HOMO/LUMO levels) of BPQs **1-3** were investigated by cyclic voltammetry, performed in deoxygenated dichloromethane at room temperature with tetrabutylammonium hexafluorophosphate (TBAPF<sub>6</sub>) as the supportive electrolyte. As shown in Figure 9 and summarized in Table 2, BPQs **2** and **3** both display an irreversible oxidation wave ( $E_{pa}$  at 1.11 V and 1.00 V, respectively) and two reversible reduction waves (half-wave potentials at -1.10 V and -1.59 V for BPQ **2** and -1.15 V and -1.60 V for BPQ **3**). Only one reversible reduction wave was observed for

BPQ **1** with  $E_{pc}$  at -1.02 V and half-wave potentials at -0.97 V. Based on their onset potential of the first oxidation and reduction waves, the HOMO-LUMO energy levels were estimated for BPQs **1-3** (HOMO energy levels of -5.49, -5.41 and -5.29 eV and LUMO energy levels of -3.49, -3.38 and -3.32 eV, respectively). Thus, the installation of alkyl groups on the pyrrolic position of these dyes indeed helps the decrease of the LUMO and the increase of the HOMO energy levels of the chromophore, and leads to the decrease of the energy band gaps. Electrochemical energy band gaps for BPQs **1-3** were calculated to be 2.00, 2.03 and 1.97 eV respectively, which are in well correlation with their optical band gaps.

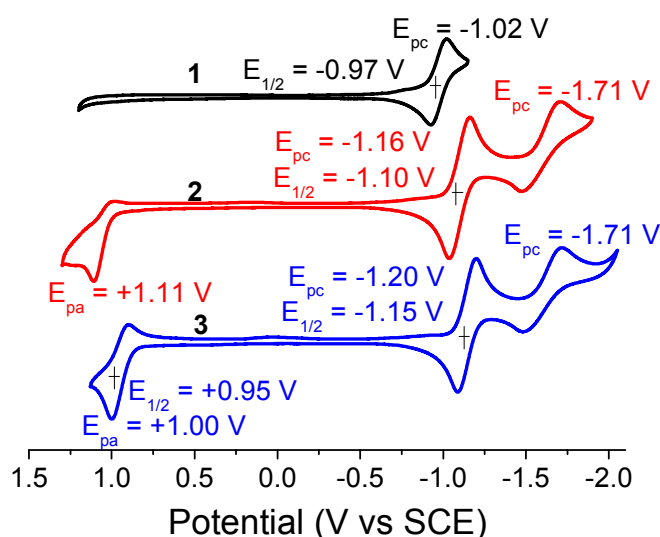


Fig. 9. Cyclic voltammograms of 1 mM BPQs **1-3** measured in dichloromethane solution, containing 0.1 M TBAPF<sub>6</sub> as the supporting electrolyte at room temperature, glassy carbon electrode as a working electrode, and the scan rate at 50 mV s<sup>-1</sup>.

Table 2. Electrochemical data acquired at 50 mV/s and HOMO-LUMO Gaps determined from spectroscopy of BPQs **1-3**.<sup>a</sup>

dyes	$E_{2^{\circ}B/B}(V)$	$E_{1^{\circ}B/B}(V)$	LUMO (eV)	HOMO (eV)	$E_g$ (eV)
<b>1</b>		-0.97	-3.49	-5.49	2.00
<b>2</b>	-1.59	-1.10	-3.38	-5.41	2.03
<b>3</b>	-1.60	-1.15	-3.32	-5.29	1.97

<sup>a</sup>  $E_{B/B}^{\circ}$  = reversible reduction potential;  $E_{red}^{onset}$  = the onset reduction potentials;  $E_{LUMO} = -e(E_{red}^{onset} + 4.4)$ ;  $E_g =$



bandgap, obtained from the intercept of the absorption spectra;  $E_{\text{HOMO}} = E_{\text{LUMO}} - E_g$ .

## Conclusions

In summary, a set of PQ ligands and their  $\text{BF}_2$  complexes (BPQs) have been efficiently synthesized from commercial reagent and showed intense yellow to deep red solid-state fluorescence. Their interesting solid-state fluorescence was interpreted by their X-ray packing structures. BPQs **2-3** both formed well ordered packing structures (slipped dimmers) due to the multiple intermolecular C-H $\cdots$ F hydrogen bonding. No intermolecular  $\pi$ - $\pi$  stacking interaction was observed in their crystal packing structures. Electrochemical energy band gaps calculated for BPQs **1-3** are in well correlation with the optical band gaps of these dyes.

## Experimental Section

**General:** Reagents and solvents were used and received from commercial suppliers unless noted otherwise. Anhydrous toluene was obtained by distillation of commercial analytical grade toluene over sodium. All reactions were performed in oven-dried or flame-dried glassware, and were monitored by TLC using 0.25 mm silica gel plates with UV indicator (60F-254).  $^1\text{H}$  and  $^{13}\text{C}$  NMR were recorded on a 300 MHz or 500 MHz NMR spectrometer at room temperature. Chemical shifts ( $\delta$ ) are given in ppm relative to  $\text{CDCl}_3$  (7.26 ppm for  $^1\text{H}$  and 77 ppm for  $^{13}\text{C}$ ) or to internal TMS. High-resolution mass spectra (HRMS) were obtained using APCI-TOF in positive mode. Electrochemical studies by cyclic voltammetry were performed with a conventional 3-electrode system using a 100 W electrochemical analyzer in deoxygenated and anhydrous dichloromethane at room temperature. Glassy carbon working electrode, the saturated calomel electrode (SCE) reference electrode, platinum auxiliary electrode, and the sample solutions contained 1 mM sample and 0.1 M tetrabutylammonium hexafluorophosphate as a supporting electrolyte were used. Argon was bubbled for 10 min before each measurement.

**Fluorometric analysis:** UV-visible absorption and fluorescence emission spectra were recorded on commercial spectrophotometers (Shimadzu UV-2450 and Edinburgh FLS920 spectrometers). All measurements were made at 25 °C, using 5 $\times$ 10 mm cuvettes. The absolute quantum yields of the

samples in solutions and solid states were measured using Edinburgh Instrument FLS920 spectrofluorimeter by calibrating sphere systems,<sup>6a</sup> excited at 500 nm for **1**, at 520 nm for **2** and **3**, and at 400 nm for **4-6**.

**X-ray crystallography for dyes 2, 3, 4 and 5:** Crystals of dyes **2-5** suitable for X-ray analysis were obtained by slow diffusion of hexane into their dichloromethane solutions. CCDC 1403580 (**2**), 1403581 (**3**), 1403582 (**4**) and 1403583 (**5**) contain the supplementary crystallographic data for this paper. These data can be obtained free of charge from The Cambridge Crystallographic Data Centre via [www.ccdc.cam.ac.uk/data\\_request/cif](http://www.ccdc.cam.ac.uk/data_request/cif). Data were collected using a diffractometer equipped with a graphite crystal monochromator situated in the incident beam for data collection at room temperature. Cell parameters were retrieved using SMART<sup>15</sup> software and refined using SAINT<sup>16</sup> on all observed reflections. The determination of unit cell parameters and data collections were performed with Mo K $\alpha$  radiation ( $\lambda$ ) at 0.71073 Å. Data reduction was performed using the SAINT software, which corrects for Lp and decay. The structure was solved by the direct method using the SHELXS-97 program and refined by least squares method on F<sup>2</sup>, SHELXL-97<sup>17</sup>, incorporated in SHELXTL V5.10<sup>18</sup>.

**General procedure for the synthesis of BPQs 1-3:** To dipyrrolylquinoxalines (0.5 mmol) in toluene (30 mL) was added 1, 8-diazabicyclo[5.4.0]undec-7-ene (DBU) (1 mL, 6.5 mmol). The mixture was refluxed for 10 min, and distilled boron trifluoride etherate (1.2 mL, 9.5 mmol) was added into the reaction mixture. The reaction mixture was refluxed for 4 h, cooled down to room temperature, poured into water and extracted with ethyl acetate. Organic layers were combined, dried over anhydrous sodium sulfate and removed under vacuum. The crude product was purified by silica gel column chromatography (hexane/dichloromethane = 2:1, v/v).

BPQ **1** was obtained as a red powder in 50% yield (77 mg) from dipyrrolylquinoxalines **4** (130 mg, 0.5 mmol). <sup>1</sup>H NMR (300 MHz, CDCl<sub>3</sub>)  $\delta$  9.63 (s, 1H), 8.12 (d,  $J$  = 8.1 Hz, 1H), 7.87 (d,  $J$  = 6.9 Hz, 1H), 7.68-7.55 (m, 2H), 7.38-7.25 (m, 3H), 7.10 (s, 1H), 6.40 (s, 2H). <sup>13</sup>C NMR (75 MHz, CDCl<sub>3</sub>)  $\delta$  143.0, 140.3, 139.9, 131.6, 130.9, 130.1, 129.5, 129.2, 128.7, 127.3, 123.2, 120.1, 118.0, 116.0, 113.9,

110.8. HRMS (APCI) Calcd. for  $C_{16}H_{12}BF_2N_4 [M + H]^+$  309.1113, found 309.1117.

BPQ **2** was obtained as a red solid in 56% yield (102 mg) from dipyrrolylquinoxalines **5** (158 mg, 0.5 mmol).  $^1H$  NMR (300 MHz,  $CDCl_3$ )  $\delta$  8.47 (s, 1H), 8.01 (d,  $J = 7.8$  Hz, 1H), 7.89 (d,  $J = 8.1$  Hz, 1H), 7.64 (t,  $J = 8.1$  Hz, 1H), 7.52 (t,  $J = 7.8$  Hz, 1H), 5.89 (s, 1H), 5.85 (s, 1H), 2.40 (s, 3H), 2.29 (s, 3H), 2.16 (s, 3H), 1.60 (s, 3H).  $^{13}C$  NMR (125 MHz,  $CDCl_3$ )  $\delta$  145.4, 145.2, 141.8, 140.4, 132.7, 132.0, 131.6, 130.8, 129.9, 129.4, 128.2, 127.4, 124.3, 119.9, 119.4, 111.5, 13.5, 13.0, 12.9, 12.5. HRMS (APCI) Calcd. for  $C_{20}H_{20}BF_2N_4 [M + H]^+$  365.1735, found 365.1739.

BPQ **3** was obtained as a red solid in 62% yield (130 mg) from dipyrrolylquinoxalines **6** (186 mg, 0.5 mmol).  $^1H$  NMR (300 MHz,  $CDCl_3$ )  $\delta$  8.34 (s, 1H), 7.86 (d,  $J = 8.1$  Hz, 1H), 7.86 (d,  $J = 8.1$  Hz, 1H), 7.60 (t,  $J = 7.5$  Hz, 1H), 7.48 (t,  $J = 7.5$  Hz, 1H), 2.43 (q,  $J = 7.5$  Hz, 1H), 2.37 (s, 3H), 2.31 (q,  $J = 7.5$  Hz, 1H), 2.24 (s, 3H), 2.12 (s, 3H), 1.50 (s, 3H), 1.08 (t,  $J = 7.5$  Hz, 1H), 1.02 (t,  $J = 7.5$  Hz, 1H).  $^{13}C$  NMR (125 MHz,  $CDCl_3$ )  $\delta$  145.5, 143.3, 141.9, 140.2, 131.9, 131.6, 130.9, 130.1, 129.3, 127.8, 127.8, 127.0, 124.2, 123.6, 122.5, 119.7, 17.9, 15.7, 15.2, 12.0, 11.7, 10.8, 10.6. HRMS (APCI) Calcd. for  $C_{24}H_{28}BF_2N_4 [M + H]^+$  421.2370, found 421.2371.

General procedure for PQs **4-6**: To dipyrrolyldiketone (1 mmol) in toluene (40 mL) was added 1, 2-phenylenediamine (216 mg, 2 mmol) and a catalytic amount of HOAc. The mixture was refluxed for 10 h, cooled down to room temperature, poured into water and extracted with ethyl acetate. Organic layers were combined, dried over anhydrous sodium sulfate and removed under vacuum. The crude product was purified by silica gel column chromatography (hexane/dichloromethane = 1:1, v/v) to give the desired products.

PQ **4**<sup>8a</sup> was synthesized as a green powder in 80% yield (208 mg) from dipyrrolyldiketone **7** (188 mg, 1 mmol).  $^1H$  NMR (300 MHz,  $CDCl_3$ )  $\delta$  9.74 (s, 2H), 7.84 (s, 2H), 7.54-7.53 (m, 2H), 6.95-6.91 (m, 4H), 6.26 (s, 2H).  $^{13}C$  NMR (75 MHz,  $CDCl_3$ )  $\delta$  143.7, 139.7, 129.1, 128.9, 128.0, 121.2, 112.9, 110.0.

PQ **5** was obtained as a brown powder in 74% yield (233 mg) from dipyrrolyldiketone **8** (244 mg, 1

mmol).  $^1\text{H}$  NMR (300 MHz,  $\text{CDCl}_3$ )  $\delta$  8.76 (s, 2H), 7.93 (q,  $J = 3.3$  Hz, 2H), 7.57 (q,  $J = 3.3$  Hz, 2H), 5.80-5.79 (m, 2H), 2.28 (s, 6H), 1.89 (s, 6H).  $^{13}\text{C}$  NMR (75 MHz,  $\text{CDCl}_3$ )  $\delta$  145.4, 139.7, 131.5, 129.1, 128.1, 125.2, 124.2, 111.6, 13.5, 12.7. HRMS (APCI) Calcd. for  $\text{C}_{20}\text{H}_{21}\text{N}_4$   $[\text{M} + \text{H}]^+$  317.1761, found 317.1760.

PQ **6** was obtained as an orange powder in 69% yield (256 mg) from dipyrrolyldiketone **9** (300 mg, 1 mmol).  $^1\text{H}$  NMR (300 MHz,  $\text{CDCl}_3$ )  $\delta$  8.52 (s, 2H), 7.88 (q,  $J = 3.3$  Hz, 2H), 7.3 (q,  $J = 3.3$  Hz, 2H), 2.37 (q,  $J = 7.5$  Hz, 4H), 2.22 (s, 6H), 1.86 (s, 6H), 1.04 (t,  $J = 7.5$  Hz, 6H).  $^{13}\text{C}$  NMR (75 MHz,  $\text{CDCl}_3$ )  $\delta$  145.8, 139.8, 128.4, 128.1, 126.6, 124.1, 123.3, 121.3, 17.5, 15.6, 11.3, 10.1. HRMS (APCI) Calcd. for  $\text{C}_{24}\text{H}_{29}\text{N}_4$   $[\text{M} + \text{H}]^+$  373.2383, found 373.2387.

**Acknowledgement.** This work is supported by the National Nature Science Foundation of China (Grants Nos. 21372011, 21402001 and 21472002), Nature Science Foundation of Anhui Province (Grants No 1508085J07) and Special and Excellent Research Fund of Anhui Normal University

**Electronic Supplementary Information (ESI) available:** Additional UV-vis, fluorescence spectra, copies of NMR spectra and high resolution mass spectra for all new compounds for dyes **2**, **3**, **4** and **5** are available in the Supporting Information. See DOI:

#### Reference:

- (1) (a) D. Li, H. Zhang and Y. Wang, *Chem. Soc. Rev.*, 2013, **42**, 8416; (b) H. Kobayashi, M. Ogawa, R. Alford, P. L. Choyke and Y. Urano, *Chem. Rev.*, 2010, **110**, 2620; (c) K. Nagura, S. Saito, R. Fröhlich, F. Glorius and S. Yamaguchi, *Angew. Chem. Int. Ed.*, 2012, **51**, 7762; (d) K. Ono, A. Nakashima, Y. Tsuji, T. Kinoshita, M. Tomura, J.-I. Nishida and Y. Yamashita, *Chem. Eur. J.*, 2010, **16**, 13539; (e) Z. Zhang, B. Xu, J. Su, L. Shen, Y. Xie and H. Tian, *Angew. Chem. Int. Ed.*, 2011, **50**, 11654; (f) M. Vendrell, D. Zhai, C. J. Er and Y.-T. Chang, *Chem. Rev.*, 2012, **112**, 4391; (g) Y. Ding, Y. Tang, W. Zhu and Y. Xie, *Chem. Soc. Rev.*, 2015, **44**, 1101; (h) H. Chen, W. Lin, W. Jiang, B. Dong, H. Cui and

Y. Tang, *Chem. Commun.*, 2015, **32**, 6968; (i) Y. Xie, P. Wei, X. Li, H. Tao, K. Zhang and H. Furuta, *J. Am. Chem. Soc.*, 2013, **135**, 19119; (j) B. Chen, G. Yu, X. Li, Y. Ding, C. Wang, Z. Liu and Y. Xie, *J. Mater. Chem. C*, 2013, **1**, 7409; (k) B. Chen, Y. Ding, X. Li, W. Zhu, J. P. Hill, K. Ariga and Y. Xie, *Chem. Commun.*, 2013, **49**, 10136.

(2) (a) D. Frath, J. Massue, G. Ulrich and R. Ziessel, *Angew. Chem. Int. Ed.*, 2014, **53**, 2290; (b) D. Frath, A. Poirel, G. Ulrich, A. De Nicola and R. Ziessel, *Chem. Comm.*, 2013, **49**, 4908; (c) D. Frath, S. Azizi, G. Ulrich and R. Ziessel, *Org. Lett.*, 2012, **14**, 4774; (d) J. Massue, D. Frath, G. Ulrich, P. Retailleau and R. Ziessel, *Org. Lett.*, 2012, **14**, 230; (e) K. Benelhadj, J. Massue, P. Retailleau, G. Ulrich and R. Ziessel, *Org. Lett.*, 2013, **15**, 2918; (f) J. Massue, D. Frath, P. Retailleau, G. Ulrich and R. Ziessel, *Chem. Eur. J.*, 2013, **19**, 5375.

(3) (a) A. Loudet and K. Burgess, *Chem. Rev.*, 2007, **107**, 4891; (b) G. Ulrich, R. Ziessel and A. Harriman, *Angew. Chem. Int. Ed.*, 2008, **47**, 1184; (c) R. Ziessel, G. Ulrich and A. Harriman, *New J. Chem.*, 2007, **31**, 496; (d) N. Boens, V. Leen and W. Dehaen, *Chem. Soc. Rev.*, 2012, **41**, 1130; (e) H. Lu, J. Mack, Y. Yang and Z. Shen, *Chem. Soc. Rev.*, 2014, **43**, 4778; (f) Y. Ni and J. Wu, *Org. Biomol. Chem.*, 2014, **12**, 3774.

(4) (a) D. Curiel, M. Ms-Montoya, L. Usea, A. Espinosa, R. A. Orenes and P. Molina, *Org. Lett.*, 2012, **14**, 3360; (b) K. Perumal, J. A. Garg, O. Blacque, R. Saiganesh, S. Kabilan, K. K. Balasubramanian and K. Venkatesan, *Chem. Asian J.*, 2012, **7**, 2670; (c) Q. D. Liu, M. S. Mudadu, R. Thummel, Y. Tao and S. N. Wang, *Adv. Funct. Mater.*, 2005, **15**, 143; (d) H. Li, W. Fu, L. Li, X. Gan, W. Mu, W. Chen, X. Duan and H. Song, *Org. Lett.*, 2010, **12**, 2924; (e) M. Mao, S. Xiao, J. Li, Y. Zou, R. Zhang, J. Pan, F. Dan, K. Zou and T. Yi, *Tetrahedron*, 2012, **68**, 5037; (f) X. Zhu, R. Liu, Y. Li, H. Huang, Q. Wang, D. Wang, X. Zhu, S. Liu and H. Zhu, *Chem. Comm.*, 2014, **50**, 12951; (g) H. Liu, H. Lu, Z. Zhou, S. Shimizu, Z. Li, N. Kobayashi and Z. Shen, *Chem. Comm.*, 2015, **51**, 1713; (h) H. Liu, H. Lu, F. Wu, Z. Li, N. Kobayashi and Z. Shen, *Org. Biomol. Chem.*, 2014, **12**, 8223.

(5) (a) C. Glotzbach, U. Kauscher, J. Voskuhl, N. S. Kehr, M. C. A. Stuart, R. Fröhlich, H. J. Galla, B. J. Ravoo, K. Nagura, S. Saito, S. Yamaguchi and E. U. Würthwein, *J. Org. Chem.*, 2013, **78**, 4410; (b) J. Häger, R. Fröhlich and E. U. Würthwein, *Eur. J. Inorg. Chem.*, 2009, **16**, 2415; (c) D. Zhao, G. Li, D. Wu, X. Qin, P. Neuhaus, Y. Cheng, S. Yang, Z. Lu, X. Pu, C. Long and J. You, *Angew. Chem. Int. Ed.*, 2013, **52**, 13676; (d) J. F. Araneda, W. E. Piers, B. Heyne, M. Parvez and R. McDonald, *Angew. Chem. Int. Ed.*, 2011, **50**, 12214; (e) C.-C. Cheng, W.-S. Yu, P.-T. Chou, S.-M. Peng, G.-H. Lee, P.-C. Wu, Y.-H. Song and Y. Chi, *Chem. Commun.*, 2003, 2628; (f) Y. Meesala, V. Kavala, H.-C. Chang, T.-S. Kuo, C.-F. Yao and W.-Z. Lee, *Dalton Trans.*, 2015, **44**, 1120; (g) Y. Yang, X. Su, C. N. Carroll and I. Aprahamian, *Chem. Sci.*, 2012, **3**, 610; (h) Y. Kubota, T. Tsuzuki, K. Funabiki, M. Ebihara and M. Matsui, *Org. Lett.*, 2010, **12**, 4010;

(6) (a) C. Yu, L. Jiao, P. Zhang, Z. Feng, C. Cheng, Y. Wei, X. Mu and E. Hao, *Org. Lett.*, 2014, **16**, 3048; (b) I.-S. Tamgho, A. Hasheminasab, J. T. Engle, V. N. Nemykin and C. J. Ziegler, *J. Am. Chem. Soc.*, 2014, **136**, 5623; (c) N. Gao, C. Cheng, C. Yu, E. Hao, S. Wang, J. Wang, Y. Wei, X. Mu and L. Jiao, *Dalton Trans.*, 2014, **43**, 7121; (d) C. Cheng, N. Gao, C. Yu, Z. Wang, J. Wang, E. Hao, Y. Wei, X. Mu, Y. Tian, C. Ran and L. Jiao, *Org. Lett.*, 2015, **17**, 278.

(7) (a) F. Szydlo, B. Andrioletti and E. Rose, *Org. Lett.*, 2006, **8**, 2345; (b) F. Szydlo, B. Andrioletti, E. Rose and C. Duhayon, *Tetrahedron Lett.*, 2004, **45**, 7363; (c) T. Ghosh, B. Maiya and A. Samanta, *Dalton Trans.*, 2006, 795; (d) L. Wang, X.-J. Zhu, W.-Y. Wong, J.-P. Guo, W.-K. Wong and Z. Y. Li, *Dalton Trans.*, 2005, 3235.

(8) (a) C. B. Black, B. Andrioletti, A. C. Try, C. Ruiperez and J. L. Sessler, *J. Am. Chem. Soc.*, 1999, **121**, 10438; (b) T. Mizuno, W. H. Wei, L. R. Eller and J. L. Sessler, *J. Am. Chem. Soc.*, 2002, **124**, 1134; (c) P. Anzenbacher, Jr., A. C. Try, H. Miyaji, V. M. Lynch, M. Matquez and J. L. Sessler, *J. Am. Chem. Soc.*, 2000, **122**, 10268; (d) S. V. Shevchuk, V. M. Lynch and J. L. Sessler, *Tetrahedron Lett.*, 2004, **60**, 11283.

- (9) (a) C.-W. Liao, R. M and S.-S. Sun, *Chem. Comm.*, 2015, **51**, 2656; (b) B. Ośmiałowski, A. Zakrzewska, B. Jędrzejewska, A. Grabarz, R. Zalesny, W. Bartkowiak and E. Kolehmainen, *J. Org. Chem.*, 2015, **80**, 2072.
- (10) (a) J. J. Klappa, S. A. Geers, S. J. Schmidtke, L. A. MacManus-Spencer and K. McNeill, *Dalton Trans.*, 2004, 883; (b) H.-Y. Chen, Y. Chi, C.-S. Liu, J.-K. Yu, Y.-M. Cheng, K.-S. Chen, P.-T. Chou, S.-M. Peng, G.-H. Lee, A. J. Carty, S.-J. Ye and C.-T. Chen, *Adv. Funct. Mater.*, 2005, **15**, 567.
- (11) G. Nawn, S. R. Oakley, M. B. Majewski, R. McDonald, B. O. Patrick and R. G. Hicks, *Chem. Sci.*, 2013, **4**, 612.
- (12) (a) O. A. Bozdemir, R. Guliyev, O. Buyukcakir, S. Selcuk, S. Kolemen, G. Gulseren, T. Nalbantoglu, H. Boyaci and E. U. Akkaya, *J. Am. Chem. Soc.*, 2010, **132**, 829; (b) X. Peng, J. Du, J. Fan, J. Wang, Y. Wu, J. Zhao, S. Sun and T. Xu, *J. Am. Chem. Soc.*, 2007, **129**, 1500; (c) E. Dai, W. Pang, X. Zhang, X. Yang, T. Jiang, P. Zhang, C. Yu, E. Hao, Y. Wei, X. Mu and L. Jiao, *Chem. Asian J.*, 2015, **10**, 1327.
- (13) (a) Q. Liu, X. Wang, H. Yan, Y. Wu, Z. Li, S. Gong, P. Liu and Z. Liu, *J. Mater. Chem. C*, 2015, **3**, 2953; (b) Y. Hong, J. W. Y. Lam and B. Z. Tang, *Chem. Comm.*, 2009, 4332.
- (14) S. Choi, J. Bouffard and Y. Kim, *Chem. Sci.*, 2014, **5**, 751.
- (15) SMART, Version 5.0, Bruker AXS, Madison, WI, USA, **1998**.
- (16) SAINT V 6.0, Bruker AXS, Madison, WI, USA, **1999**.
- (17) SHELXL-97, Program for X-ray Crystal Structure Solution, University of Gottingen, Germany, **1997**.
- (18) SHELXTL v5.10, Program Library for Structure Solution and Molecular Graphics, Bruker AXS, Madison, WI, **1998**.